Available online at www.sciencedirect.com
SCIENCE DIRECT®
International Journal of Heat and Mass Transfer 48 (2005) 2172–2185
International Journal of HEAT and MASS TRANSFER
www.elsevier.com/locate/ijhmt

Heat transfer enhancement through control of thermal dispersion effects

A.-R.A. Khaled, K. Vafai *

Department of Mechanical Engineering, University of California, A363 Bourns Hall, Riverside, CA 92521-0425, USA

Received 18 June 2004; received in revised form 31 December 2004
Available online 13 March 2005

Abstract

Heat transfer enhancements are investigated inside channels by controlling thermal dispersion effects inside the fluid. Different distributions for the dispersive elements such as nanoparticles or flexible hairy fins extending from the channel plates are considered. Energy equations for different fluid regions are dimensionalized and solved analytically and numerically. The boundary arrangement and the exponential distribution for the dispersive elements are found to produce enhancements in heat transfer compared to the case with a uniform distribution for the dispersive elements. The presence of the dispersive elements in the core region does not affect the heat transfer rate. Moreover, the maximum Nusselt number for analyzed distributions of the dispersive elements are found to be 21% higher than that with uniformly distributed dispersive elements for a uniform flow. On the other hand, the parabolic velocity profile is found to produce a maximum Nusselt number that is 12% higher than that with uniformly distributed dispersive elements for the boundary arrangement. The distribution of the dispersive elements that maximizes the heat transfer is governed by the flow and thermal conditions plus the properties of the dispersive elements. Results in this work point towards preparation of super nanofluids or super dispersive media with enhanced cooling characteristics.

Keywords: Thermal dispersion; Nanofluid; Heat transfer; Dispersive elements; Enhancement

1. Introduction

The heat flux of VLSI microelectronic components can reach up to 1000 kW/m^2. As such, many methods are proposed to eliminate excess of heating associated with the operation of these components. One of these methods is to utilize two-layered microchannels [1]. Two-phase flow are utilized for cooling which was found to be capable of removing maximum heat fluxes generated by electronic packages yet the system may become unstable near certain operating conditions. This can be shown in the work of Bowers and Mudawar [2]. The use of porous blocks inside channels [3–5] was found to be efficient in eliminating the excess of heat. However, the porous medium creates a substantial increase in the pressure drop inside the cooling device. Recently, Khaled and Vafai [6] demonstrated that expandable systems can provide an efficient method for enhancing the cooling rate. The performance of expandable systems and other cooling systems can be further improved when nanofluids are used as their coolants [6–9].

Nanofluids are mixtures of a pure fluid with a small volume of suspensions of ultrafine particles such as

* Corresponding author. Tel.: +1 951 827 2135; fax: +1 951 827 2899.
E-mail address: vafai@engr.ucr.edu (K. Vafai).

0017-9310/$ - see front matter © 2005 Elsevier Ltd. All rights reserved.
doi:10.1016/j.ijheatmasstransfer.2004.12.035

Nomenclature

B	channel length
C^*	dispersive coefficient (dependent on the dispersive elements properties)
c_p	average specific heat
E_0	thermal dispersion parameter
h	half channel height
h_c	convective heat transfer coefficient
k	thermal conductivity
k_0	effective static thermal conductivity of the nanofluid
Nu	Nusselt number
Nu_{fd}	Nusselt number at fully developed condition
Pe	Peclet number
q	heat flux at the channel walls
T, T_1	fluid's temperature and the inlet temperature
U, u	dimensionless and dimensional axial velocities
X, x	dimensionless and dimensional axial coordinates
Y, y	dimensionless and dimensional normal coordinates

Greek symbols

θ, θ_m	dimensionless temperature and dimensionless mean bulk temperature
θ_W	dimensionless temperature of the channel plates
ρ	density

Subscripts

f	pure fluid
nf	nanofluid
p	particle

copper nanoparticles or nanotubes. They were found to possess a large effective thermal conductivity. For example, the effective thermal conductivity of nanofluids could reach 1.5 times that of the pure fluid when the volume fraction of the copper nanoparticles is 0.003 [10]. This enhancement is expected to be further increased as the flow speed increases resulting in an increase in the mixing effects associated with the Brownian motion of the nanoparticles. This mixing effect is referred in literature as the thermal dispersion effect [11]. Other aspects of dispersion effects can be found in some of the recent works [12–17]. Li and Xuan [18] reported an increase of 60% in the convective heat transfer inside a channel filled with a nanofluid, having 3% volume fraction for copper nanoparticles, compared to its operation with the pure fluid. This significant increase indicates that thermal dispersion is the main mechanism for heat transfer inside convective flows. The challenge is to find new ways to improve the performance of the cooling systems.

In this work, a method for enhancing the heat transfer characteristics through the use of nanofluids with proper thermal dispersion properties is proposed and analyzed. This can be accomplished by having a proper distribution for the ultrafine particles. Physically, the distribution of the ultrafine particles can be controlled using different methods: (i) having nanoparticles with different sizes or physical properties, (ii) applying appropriate magnetic forces along with using magnetized nanoparticles, (iii) applying appropriate centrifugal forces, and (iv) applying appropriate electrostatic forces along with using electrically charged nanoparticles. Different distribution for the nanoparticles can be obtained using any combination of the above methods.

For example, denser nanoparticles such as copper nanoparticles or those with a larger size tend to suspend at lower altitudes in coolants. However, nanoparticles with lower density such as carbon nanoparticles or those having a lower size tend to swim at higher altitudes within denser liquids such as aqueous solutions and liquid metals. As such, non-homogenous thermal dispersion properties can be attained. Centrifugal effects tend to produce concentrated thermal dispersion properties near at least one of the boundaries. On the other hand, non-homogenous thermal dispersion properties inside the coolant can be obtained by attaching to the plates of the cooling device flexible thin fins like hair with appropriate lengths. The Brownian motion of the suspended hairy medium will increase the thermal dispersion properties mainly near the plates of the cooling device and it can be used with a proper suspension system to obtain any required thermal dispersion properties.

Heat transfer enhancements are analyzed inside a channel filled with a coolant having different thermal dispersion properties. Different arrangements for the nanoparticles or the dispersive elements are considered in this work. The nanoparticles or the dispersive elements are considered to be uniformly distributed near the center of the channel for one of the arrangements. In another arrangement, they are uniformly distributed near the channel plates. Exponential or parabolic distributions for the dispersive elements are also analyzed in this work. The energy equations for the corresponding fluid regions are non-dimensionalized. Solutions for the Nusselt number and the temperature are obtained analytically for special cases and numerically for general cases. They are utilized to determine the appropriate

distribution for the dispersive elements that will result in the maximum heat transfer with the same total number of nanoparticles or the dispersive elements.

2. Problem formulation

Consider a flow inside a two-dimensional channel with a height $2h$ and a length B. The x-axis is aligned along the centerline of the channel while the y-axis is in the traverse direction as shown in Fig. 1. The fluid which could be a pure fluid or a nanofluid is taken to be Newtonian with constant average properties except for the thermal conductivity to account for thermal dispersion effects. The energy equation is

$$\rho c_p u \frac{\partial T}{\partial x} = \frac{\partial}{\partial y}\left(k \frac{\partial T}{\partial y}\right) \tag{1}$$

where T, ρ, c_p and k are the temperature, effective fluid density, fluid specific heat and thermal conductivity, respectively. The velocity field u in the channel is taken to be fully developed. The volume of the dispersive elements is very small such that the velocity profile is parabolic.

$$\frac{u}{u_m} = \frac{3}{2}\left(1 - \left(\frac{y}{h}\right)^2\right) \tag{2}$$

where u_m is the mean flow speed.

For nanofluids or in the thermally dispersed region, the parameter ρc_p will be $(\rho c_p)_{nf}$ and it is equal to

$$(\rho c_p)_{nf} = (1-\varphi)(\rho c_p)_f + \varphi(\rho c_p)_p \tag{3}$$

where the subscript nf, f and p denote the nanofluid or the dispersive region, pure fluid and the particles, respectively. The parameter φ is the nanoparticles or the dispersive elements volume fraction which represents the ratio of the nanoparticles or the dispersive elements volume to the total volume. A nanofluid composed of pure water and copper nanoparticles suspensions with 2% volume fraction has a value of $(\rho c_p)_{nf}$ equal to 99% that for the pure water which is almost the same as the thermal capacity of the pure fluid.

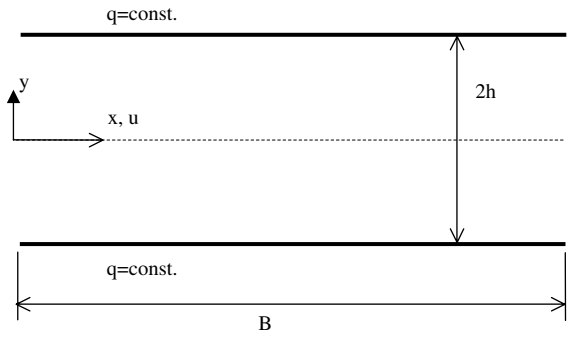

Fig. 1. Schematic diagram and the coordinate system.

The ultrafine suspensions such as nanoparticles, nanotubes or any dispersive elements in the fluid plays an important role in heat transfer inside the channel as their Brownian motions tend to increase fluid mixing. This enhances the heat transfer. The correlations presented in the work of Li and Xuan [18] for Nusselt numbers in laminar or turbulent flows show that the heat transfer is enhanced in the presence of nanoparticles and it increases as the nanoparticles volume fraction, the diameter of the nanoparticles or the flow speed increase. Xuan and Roetzel [11] suggest (consistent with the dispersion model given in [17]) the following linearized model for the effective thermal conductivity of the nanofluid:

$$k = k_0 + C^*(\rho c_p)_{nf}\varphi h u \tag{4}$$

where C^* is a constant depending on the diameter of the nanoparticle and its surface geometry. Physically, Eq. (4) is a first approximation for the thermal conductivity of the nanofluid that linearly relates it to thermal capacitance of the flowing nanoparticles or flowing dispersive elements. The constant k_0 represents the effective thermal conductivity of the nanofluid or the dispersive region under stagnant conditions, at $u = 0$. This constant can be predicted for nanofluids from the formula suggested by Wasp [19] which has the following form:

$$\frac{k_0}{k_f} = \frac{k_p + 2k_f - 2\varphi(k_f - k_p)}{k_p + 2k_f + 2\varphi(k_f - k_p)} \tag{5}$$

where k_p and k_f are the thermal conductivity of the nanoparticles and the pure fluid, respectively.

According to formula (5), a 2% volume fraction of ultrafine copper particles produces 8% increase in k_0 when compared to the thermal conductivity of the pure fluid. On the other hand, the experimental results illustrated in the work of Li and Xuan [18] shows that the presence of suspended copper nanoparticles with 2% volume fraction produced about 60% increase in the convective heat transfer coefficient compared to pure fluid (Table 1). This indicates that thermal dispersion is the main mechanism for enhancing heat transfer inside channels filled with nanofluids under convective conditions. Non-dimensionalizing Eq. (1) with the following dimensionless variables:

$$X = \frac{x}{h}, \quad Y = \frac{y}{h}, \quad U = \frac{u}{u_m}, \quad \theta = \frac{T - T_1}{qh/k_f} \tag{6}$$

leads to the following dimensionless energy equation:

$$PeU\frac{\partial \theta}{\partial X} = \frac{\partial}{\partial Y}\left(\frac{k}{k_f}\frac{\partial \theta}{\partial Y}\right) \tag{7}$$

where q, T_1 and Pe are the heat flux at the channel's plates, the inlet temperature and the Peclet number

Table 1
Variations of $(\rho c_p)_{nf}/(\rho c_p)_f$ and k_0/k_f for various ultrafine copper particles volume ratios

φ (%)	$(\rho c_p)_{nf}/(\rho c_p)_f$	k_0/k_f
0	1	1
1	0.998	1.040
2	0.996	1.083
3	0.995	1.127
4	0.993	1.173
5	0.991	1.221

($Pe = (\rho c_p u_m h)/k_f$), respectively. It is assumed that the heat flux is constant and equal at both plates.

For simplicity, the term k/k_f will be rearranged in the following form:

$$\frac{k}{k_f} = \frac{k_0}{k_f} + \lambda \frac{(\rho c_p)_{nf}}{(\rho c_p)_f} \varphi U_{nf}, \quad \lambda = C^* Pe_f \tag{8}$$

where $Pe_f = (\rho c_p)_f u_m h/k_f$.

A portion of the fluid's volume are considered in part of this work to be subjected to thermal dispersion effects due the suspensions of nanoparticles or any dispersive elements while the other portion contains only the pure fluid. The most obvious way to obtain specific distributions for thermal dispersive elements is to have conductive hairy fins extending from the channel plates or from a carefully designed fixed or flexible structure placed in the channel. The volume of this structure is small enough such that the parabolic assumption for the velocity profile is still valid. Also, non-homogenous thermal dispersion properties can be achieved by having nanoparticles with different densities or different sizes. Heavier nanoparticles or dispersive elements tend to swim closer to the lower plate due to gravitational forces while lighter nanoparticles or dispersive elements tend to swim closer to the upper force due to buoyancy forces. The dispersive elements such as nanoparticles can be further concentrated near the channel's plates by having these particles magnetized along with applying appropriate magnetic fields. As such, the difference in the thermal dispersive properties of the nanofluid can be achieved. Appropriate thermal dispersive properties can be obtained by utilizing the different methods discussed in Section 1.

The dimensionless energy equation for the part involving thermal dispersion is

$$(Pe)_f \left(\frac{(\rho c_p)_{nf}}{(\rho c_p)_f}\right) U_{nf} \frac{\partial \theta_{nf}}{\partial X} = \frac{\partial}{\partial Y}\left(\left(\frac{k_0}{k_f} + \lambda \frac{(\rho c_p)_{nf}}{(\rho c_p)_f} \varphi U_{nf}\right) \frac{\partial \theta_{nf}}{\partial Y}\right) \tag{9}$$

while the energy equation for the volume containing the pure fluid is

$$(Pe)_f U_f \frac{\partial \theta_f}{\partial X} = \frac{\partial^2 \theta_f}{\partial Y^2} \tag{10}$$

Different distributions for the nanoparticles of the dispersive elements will be analyzed in this work. In one of these distributions, the region that is active with thermal dispersion effects is considered to be a rectangular region of height 2ℓ around the channel's centerline as shown in Fig. 2(a). Another distribution considers the region comprising thermal dispersion effects to be present only at the two identical rectangular regions of height ℓ attached to the channel's plates as shown in Fig. 2(b). The boundary conditions for the central arrangement are

$$\frac{d\theta_{nf}(X,0)}{dY} = 0, \left(\frac{k_0}{k_f} + \lambda \frac{(\rho c_p)_{nf}}{(\rho c_p)_f} \varphi U(\Lambda)\right) \frac{d\theta_{nf}(X,\Lambda)}{dY} = \frac{d\theta_f(X,\Lambda)}{dY}, \theta_f(X,\Lambda) = \theta_{nf}(X,\Lambda), \frac{d\theta_f(X,1)}{dY} = 1 \tag{11a–d}$$

while the boundary conditions for the second arrangement (boundary arrangement) are

$$\frac{d\theta_f(X,0)}{dY} = 0,$$
$$\left(\frac{k_0}{k_f} + \lambda \frac{(\rho c_p)_{nf}}{(\rho c_p)_f} \varphi U(1-\Lambda)\right) \frac{d\theta_{nf}(X,1-\Lambda)}{dY} = \frac{d\theta_f(X,1-\Lambda)}{dY},$$
$$\theta_f(X,1-\Lambda) = \theta_{nf}(X,1-\Lambda),$$
$$\left(\frac{k_0}{k_f} + \lambda \frac{(\rho c_p)_{nf}}{(\rho c_p)_f} \varphi U(1)\right) \frac{d\theta_f(X,1)}{dY} = 1 \tag{12a–d}$$

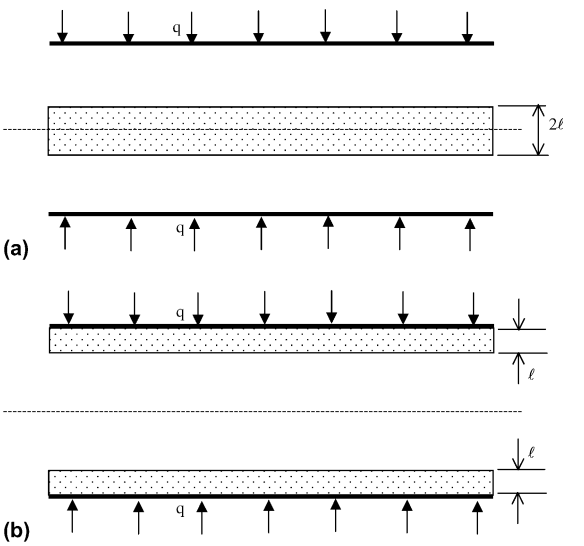

Fig. 2. Different arrangements for the thermal dispersion region: (a) central arrangement, and (b) boundary arrangement.

where $\Lambda = \ell/h$. Other distributions for the dispersive elements will be considered later such as the parabolic distribution and the exponential distribution.

For thermal fully developed conditions, axial gradient of the temperature reaches a constant value equal to $\mathrm{d}T/\mathrm{d}x$. That is, the heat flux is equal to

$$q = \frac{\mathrm{d}T}{\mathrm{d}x}\left((1-\varphi_{\mathrm{cf}})(\rho c_p)_{\mathrm{f}}(u_{\mathrm{m}})_{\mathrm{f}} + \varphi_{\mathrm{cf}}(\rho c_p)_{\mathrm{nf}}(u_{\mathrm{m}})_{\mathrm{nf}}\right)h \quad (13)$$

where φ_{cf} is the ratio of the volume comprising thermal dispersion effects to the total channel volume. $(u_{\mathrm{m}})_{\mathrm{f}}$ is the average velocity in the fluid phase while $(u_{\mathrm{m}})_{\mathrm{nf}}$ is the average velocity in the nanofluid or the region containing the thermal dispersive elements. As such, Eqs. (9) and (10) reduce to

$$AU_{\mathrm{nf}} = \frac{\partial}{\partial Y}\left((K + E\varphi U)\frac{\partial\theta_{\mathrm{nf}}}{\partial Y}\right) \quad (14)$$

$$GU_{\mathrm{f}} = \frac{\partial^2\theta_{\mathrm{f}}}{\partial Y^2} \quad (15)$$

where $A = Pe_{\mathrm{f}}\left(\frac{(\rho c_p)_{\mathrm{nf}}}{(\rho c_p)_{\mathrm{f}}}\right)\frac{\mathrm{d}\theta_{\mathrm{nf}}}{\mathrm{d}X}$, $K = k_0/k_{\mathrm{f}}$, $E = \lambda\frac{(\rho c_p)_{\mathrm{nf}}}{(\rho c_p)_{\mathrm{f}}}\varphi$ and $G = (Pe)_{\mathrm{f}}\frac{\mathrm{d}\theta_{\mathrm{f}}}{\partial X}$. Since $(\rho c_p)_{\mathrm{nf}}$ does not vary significantly when the volume fraction of the ultrafine particles or the dispersive elements is less than 4% as used in the literature, A and G are almost equal to unity

$$\left(Pe_{\mathrm{f}}\frac{\mathrm{d}\theta}{\mathrm{d}X} = \left(\frac{\rho c_p u_{\mathrm{m}} h}{k}\right)\frac{\mathrm{d}(Tk/(qh))}{\mathrm{d}(x/h)} = \frac{\rho c_p u_{\mathrm{m}} h}{q}\frac{\mathrm{d}T}{\mathrm{d}x} = 1.0\right).$$

3. Analytical solutions

Consider a uniform flow inside the channel such that $U = 1$. Eqs. (14) and (15) reduce to

$$\frac{\partial^2\theta_{\mathrm{nf}}}{\partial Y^2} = \frac{1}{(K+E)}, \quad \frac{\partial^2\theta_{\mathrm{f}}}{\partial Y^2} = 1 \quad (16a,b)$$

The solution to Eqs. (16a) and (16b) for the central arrangement of the dispersive elements is

$$\frac{\theta_W(X) - \theta_{\mathrm{nf}}(X,Y)}{\theta_W(X) - \theta_{\mathrm{m}}(X)} \cong \frac{1.5\left(\Lambda^2 - Y^2\right) + 1.5(K+E)\left(1-\Lambda^2\right)}{\Lambda^3 - (K+E)\left(\Lambda^3 - 1.5\Lambda^2 + 0.5\right) + 1.5(K+E)\left(1-\Lambda^2\right)}, \quad 0 < Y < \Lambda \quad (17a)$$

$$\frac{\theta_W(X) - \theta_{\mathrm{f}}(X,Y)}{\theta_W(X) - \theta_{\mathrm{m}}(X)} \cong \frac{1.5\left(1-Y^2\right)(K+E)}{\Lambda^3 - (K+E)\left(\Lambda^3 - 1.5\Lambda^2 + 0.5\right) + 1.5(K+E)\left(1-\Lambda^2\right)}, \quad \Lambda < Y < 1 \quad (17b)$$

where θ_{w} is the plate temperature at a given section X. The parameter θ_{m} is the mean bulk temperature. It is defined as

$$\theta_{\mathrm{m}}(X) = \int_0^1 U(Y)\theta(X,Y)\,\mathrm{d}Y \quad (18)$$

As such, the fully developed value for the Nusselt number is

$$Nu_{\mathrm{fd}} = \frac{h_{\mathrm{c}}h}{k_{\mathrm{f}}} = \frac{1}{\theta_W(X) - \theta_{\mathrm{m}}(X)} = \frac{1}{\theta_{\mathrm{f}}(X,1) - \theta_{\mathrm{m}}(X)} \cong \frac{3(K+E)}{\Lambda^3 - (K+E)\left(\Lambda^3 - 1.5\Lambda^2 + 0.5\right) + 1.5(K+E)\left(1-\Lambda^2\right)} \quad (19)$$

where h_{c} is the convective heat transfer coefficient at the channel's plate.

For the second type of arrangements for the thermal dispersion region. The solution for Eqs. (16a) and (16b) is

$$\frac{\theta_W(X) - \theta_{\mathrm{f}}(X,Y)}{\theta_W(X) - \theta_{\mathrm{m}}(X)} \cong \frac{1.5\left(1 + \left(1-\Lambda^2\right)(K+E)\left(1-Y^2\right) - \left(1-\Lambda\right)^2\right)}{K - (K-1)\left(\Lambda^3 - 3\Lambda^2 + 3\Lambda\right) + E\left(1-\Lambda\right)^3}, \quad 0 < Y < \Lambda \quad (20a)$$

$$\frac{\theta_W(X) - \theta_{\mathrm{nf}}(X,Y)}{\theta_W(X) - \theta_{\mathrm{m}}(X)} \cong \frac{1.5\left(1-Y^2\right)}{K - (K-1)\left(\Lambda^3 - 3\Lambda^2 + 3\Lambda\right) + E\left(1-\Lambda\right)^3}, \quad \Lambda < Y < 1 \quad (20b)$$

The corresponding fully developed value for Nusselt number for this case is

$$Nu_{\mathrm{fd}} = \frac{h_{\mathrm{c}}h}{k_{\mathrm{f}}} = \frac{1}{\theta_W(X) - \theta_{\mathrm{m}}(X)} = \frac{1}{\theta_{\mathrm{nf}}(X,1) - \theta_{\mathrm{m}}(X)} \cong \frac{3(K+E)}{K - (K-1)\left(\Lambda^3 - 3\Lambda^2 + 3\Lambda\right) + E\left(1-\Lambda\right)^3} \quad (21)$$

3.1. Volume fraction of the dispersive elements

The total number of dispersive elements is considered to be fixed for each distribution. As such, the volume fraction of the dispersive element for the central or the boundary arrangements is related to their thickness according to the following relation:

$$\varphi = \frac{\varphi_0 h}{\ell} = \frac{\varphi_0}{\Lambda} \quad (22)$$

where φ_0 is the volume fraction of the dispersive elements when they are uniformly filling the whole channel volume. Utilizing Eq. (22), the parameter E utilized in

Eqs. (14) and (15a) can be expressed according to the following:

$$E = E_0\left(\frac{h}{\ell}\right) = \frac{E_0}{\Lambda} \tag{23}$$

where E_0 is named as the thermal dispersion parameter.

3.2. Other spatial distribution for the dispersive elements

Practically, it is difficult to have the dispersive elements concentrated in a region while the other region is a pure fluid. As such, two other distributions for the dispersive elements are considered in this work. They are the exponential and the parabolic distributions as illustrated in the following:

$$\varphi = \varphi_0\left(1 + D_c\left(\frac{1}{3} - \left(\frac{y}{h}\right)^2\right)\right) \tag{24}$$

$$\varphi = \frac{\varphi_0 D_e}{e^{D_e} - 1} e^{D_e Y} \tag{25}$$

Note that the average volume fraction for each distribution is φ_0 irrespective to values of D_e and D_p. One of the objectives of our work is to obtain the values of D_c and D_e and Λ that produces maximum heat transfer inside the channel.

The excess in Nusselt number κ is defined as the ratio of the maximum Nusselt number that can be obtained by having a certain volume fraction distribution (Nu_{nd}) to the Nusselt number corresponding to a uniform distribution of the dispersive elements (Nu_{ud}). It is expressed as follows:

$$\kappa = \frac{Nu_{nd}}{Nu_{ud}} \tag{26}$$

It can be shown that Eq. (26) exhibits a local maximum or minimum value at specific thermal dispersion parameter $(E_0^*)_{critical}$ for the boundary arrangement. This is related to the dimensionless thickness of the dispersive region through the following relation:

$$\frac{(E_0^*)_{critical}}{K\Lambda} = -1 + \sqrt{\frac{\left(K\left(\Lambda^3 - 3\Lambda^2 + 3\right) + (1-\Lambda)(\Lambda - 2)\right)}{(1-\Lambda)^3}} \tag{27}$$

4. Numerical methods

Eqs. (9) and (10) were discritized using three points central differencing in the Y direction while backward differencing was utilized for the temperature gradient in the X-direction. The resulting tri-diagonal system of algebraic equations at $X = \Delta X$ was then solved utilizing the well-established Thomas algorithm [20]. The same procedure was repeated for the consecutive X-values until X reached the value of B/h. Eqs. (13) and (14) were also discritized using three points central differencing and solved using Thomas algorithm.

5. Discussion

5.1. Thermal dispersion effects for the central and boundary arrangements

Fig. 3 shows the variation of the fully developed Nusselt number with the thermal dispersion parameter E_0 and the dimensionless thickness of the thermally dispersed region Λ for the central arrangement. For lower values of Λ, the Nusselt number does not change due to concentrations of the thermal dispersive elements around the center of the channel. However, as the thickness of the dispersive region increases, it will have a profound effect on the Nusselt number. The motion of nanoparticles or the dispersive elements within the core flow of the channel produces a negligible change in the heat transfer characteristics as shown in Fig. 3. The Nusselt number increases as Λ increases to a maximum value and then starts to decrease when the dispersive elements are concentrated according to the boundary arrangement (Fig. 4). The arrangement shown in Fig. 4 illustrates that a specific distribution for the same dispersive elements can enhance the heat transfer. This distribution is a function of E_0 and the velocity profile as shown in Fig. 4. In this figure, the thermal dispersive region thickness Λ that produces the optimum enhancement in the Nusselt number is shown to increase as the E_0 increases. As such, flow and thermal conditions along with the properties of the dispersive elements such as their sizes and their surface geometry determine the distribution of the dispersive elements that result in a maximum enhancement in the heat transfer.

5.2. Thermal dispersion effects for the central and boundary arrangements at thermally developing conditions

Fig. 5 illustrates the effects of the dispersion coefficient C^* on the Nusselt number at the exit for various thicknesses of the thermally dispersed region Λ arranged with the central configuration. These values are for a thermally developing condition as the minimum Nusselt number in this figure is greater than the corresponding value at thermally developed conditions illustrated in Fig. 3. This figure shows that when Λ is below 0.35, heat transfer is almost unaffected by thermal dispersion. As can be seen, the average plate temperature shown in Fig. 6 ($Pe_f = 670$) is almost unchanged when Λ is below 0.37 while it is below 0.5 in Fig. 7 ($Pe_f = 1340$) for the

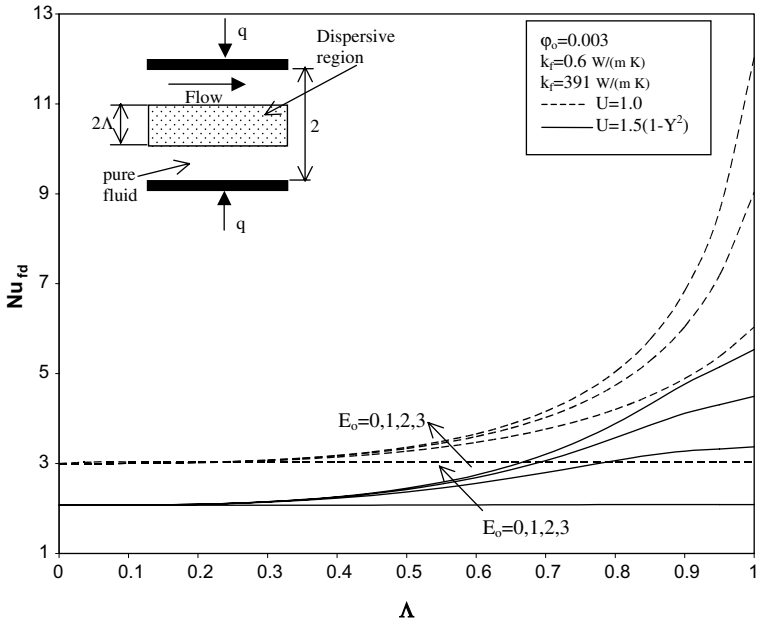

Fig. 3. Effects of the thermal dispersion parameter E_0 and the dimensionless thickness Λ on the Nusselt number at thermally fully developed conditions for the central arrangement (the number of the dispersive elements is the same for each arrangement).

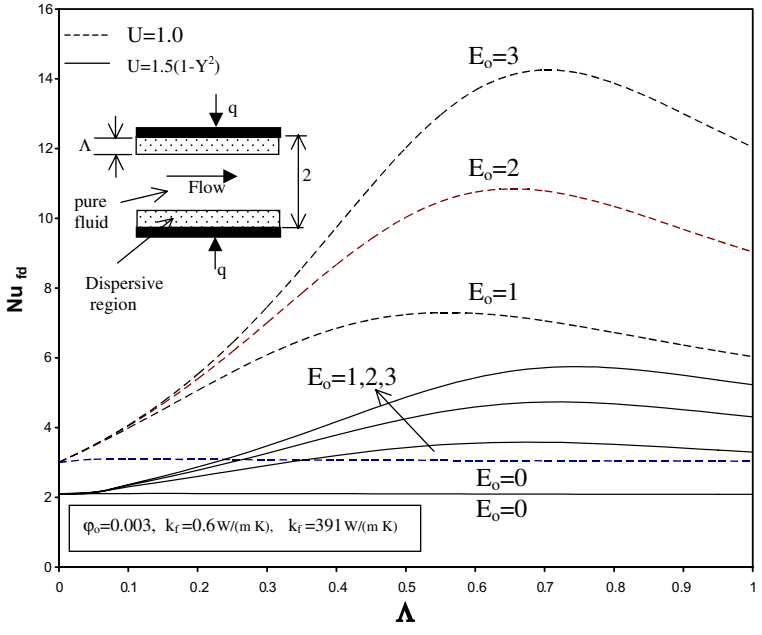

Fig. 4. Effects of the thermal dispersion parameter E_0 and the dimensionless thickness Λ on the Nusselt number at thermally fully developed conditions for the boundary arrangement (the number of the dispersive elements is the same for each arrangement).

central arrangement. Similarly, the maximum Nusselt number or the minimum average plate temperatures at lower Pe_f values occur at higher values of Λ compared to those at higher Pe_f values for different boundary arrangements as can be noticed from Figs. 4, 8–10. This is because temperature gradients near the core flow increase as Pe_f decreases thus thermal dispersion effects are increased.

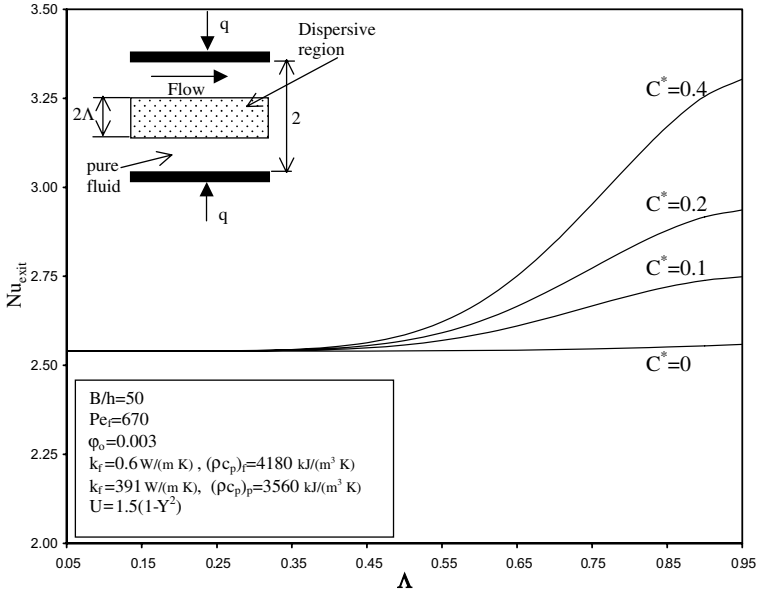

Fig. 5. Effects of the dispersion coefficient C^* and the dimensionless thickness Λ on the Nusselt number at the exit for central arrangement (the number of the dispersive elements is the same for each arrangement).

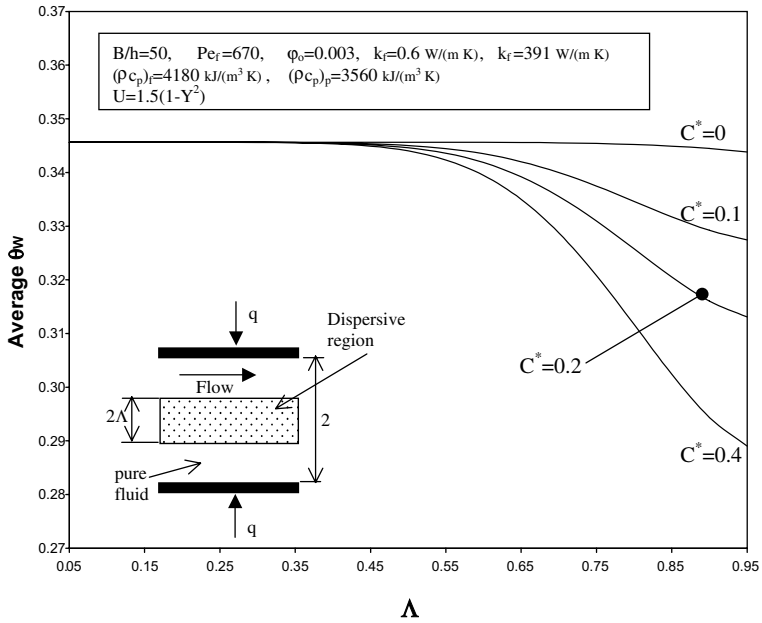

Fig. 6. Effects of the dispersion coefficient C^* and the dimensionless thickness Λ on the average dimensionless plate temperature θ_W for central arrangement (the number of the dispersive elements is the same for each arrangement, $Pe_f = 670$).

5.3. Thermal dispersion effects on the excess in the Nusselt number at thermally fully developed conditions

Figs. 11 and 12 illustrate various proposed volume fraction distributions for the same nanoparticles. As shown in Fig. 13, the Nusselt number reaches a maximum value when $E_0 > 0$ for the exponential distribution of the dispersive elements while the parabolic distribution produces no maxima in the Nusselt number (Fig. 14). The excess in Nusselt number κ is always greater

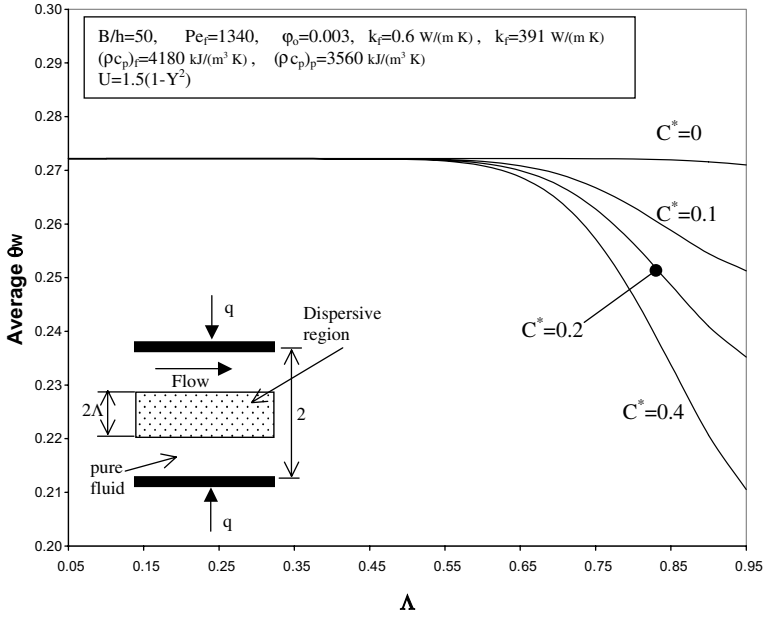

Fig. 7. Effects of the dispersion coefficient C^* and the dimensionless thickness Λ on the average dimensionless plate temperature θ_W for central arrangement (the number of the dispersive elements is the same for each arrangement, $Pe_f = 1340$).

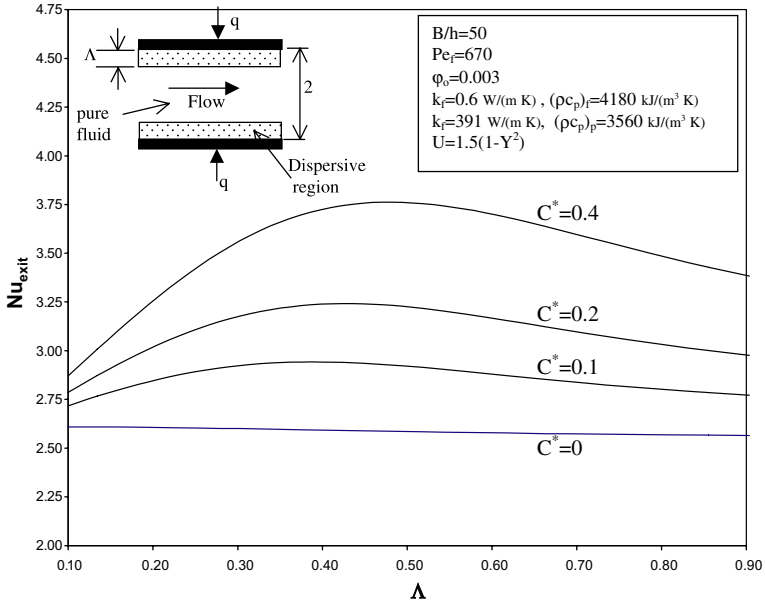

Fig. 8. Effects of the dispersion coefficient C^* and the dimensionless thickness Λ on the Nusselt number at the exit for the boundary arrangement (the number of the dispersive elements is the same for each arrangement).

than one for the boundary arrangement while it is greater than one for the exponential distribution when the velocity is uniform as shown in Fig. 15. The excess in Nusselt number increases as E_0 increases and reaches a constant value equal to 1.12 for the parabolic velocity profile along with the boundary arrangement for the dispersive elements while it is 1.21 for the uniform velocity profile. This indicates that almost 12% increase in the

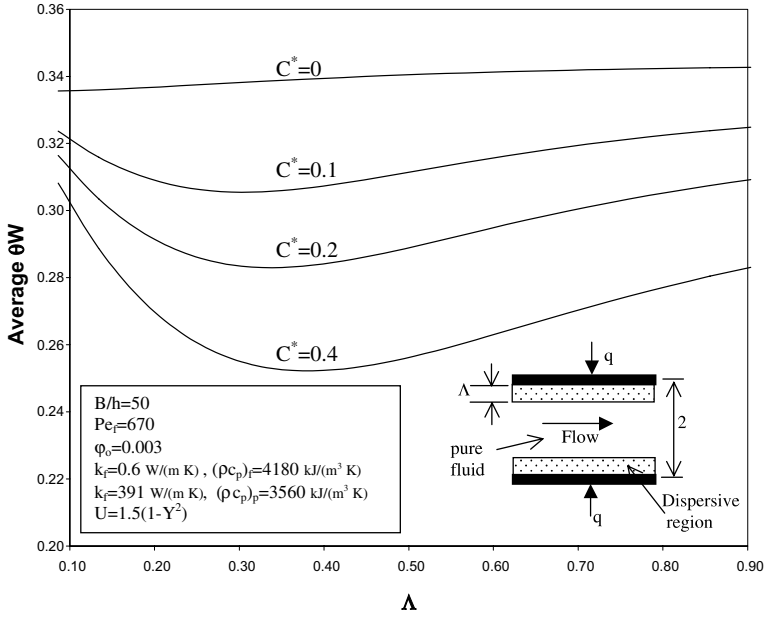

Fig. 9. Effects of the dispersion coefficient C^* and the dimensionless thickness Λ on the average dimensionless plate temperature θ_W for boundary arrangement (the number of the dispersive elements is the same for each arrangement, $Pe_f = 670$).

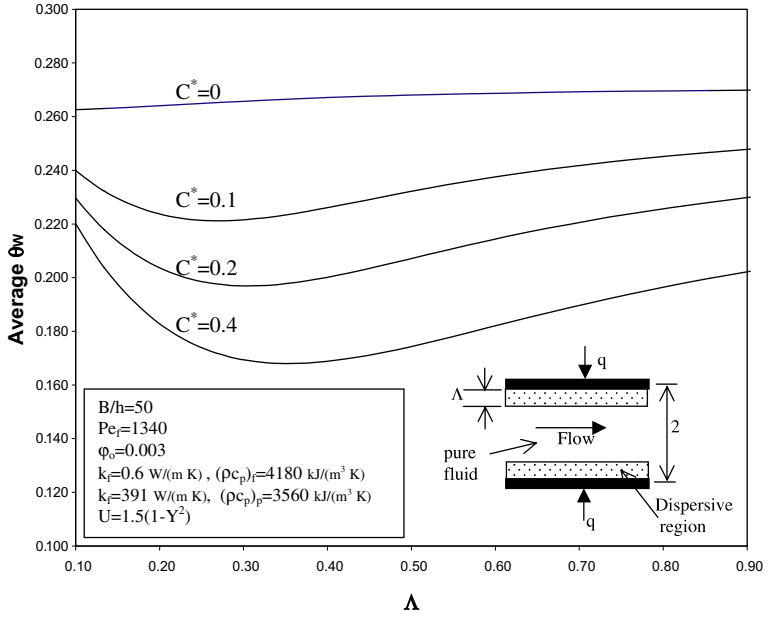

Fig. 10. Effects of the dispersion coefficient C^* and the dimensionless thickness Λ on the average dimensionless plate temperature θ_W for boundary arrangement (the number of the dispersive elements is the same for each arrangement, $Pe_f = 1340$).

heat transfer can be achieved in highly dispersive media when the dispersive elements are concentrated near the boundary for the parabolic velocity profile. The exponential distribution produced a maximum excess in the Nusselt number equal to 1.18 for uniform velocity profile. The latter results can be used to model Darcian flow inside a channel filled with a porous medium having a uniform porosity and comprising dispersive elements

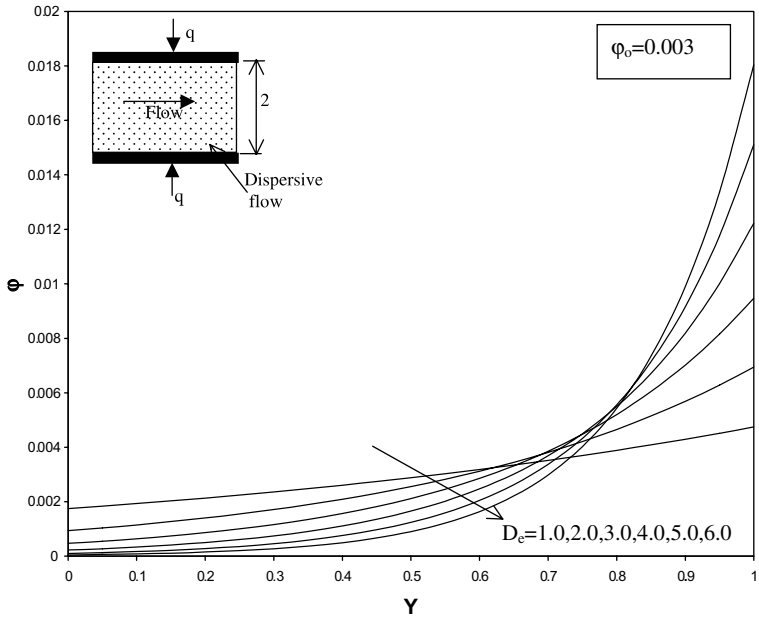

Fig. 11. Effects of D_e on the volume fraction distribution of the dispersive element (the number of the dispersive elements is the same for each distribution).

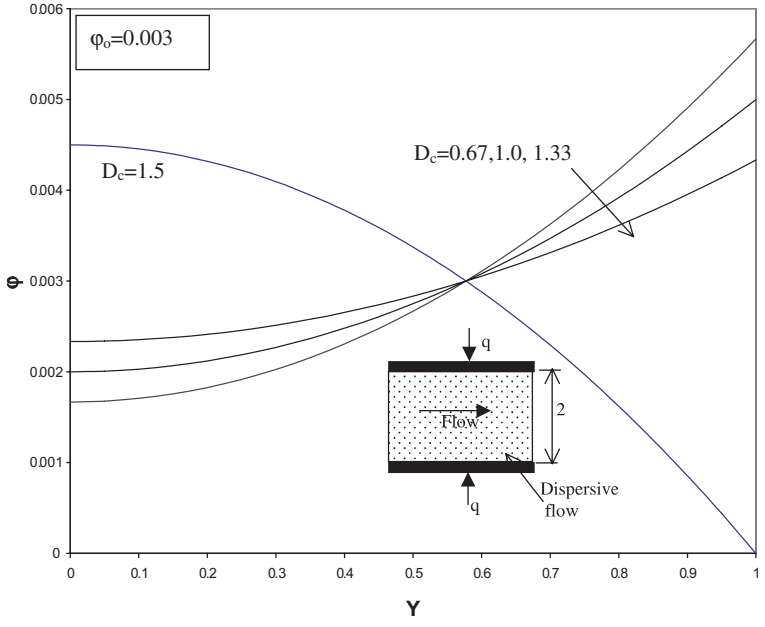

Fig. 12. Effects of D_c on the volume fraction distribution of the dispersive elements (the number of the dispersive elements is the same for each distribution).

exponentially distributed along the center line of the channel. These figures illustrate the importance of flow conditions and the distribution of the dispersive elements on the degree of enhancement in heat transfer.

6. Conclusions

Enhancements in heat transfer are investigated inside channels filled with a fluid having different thermal

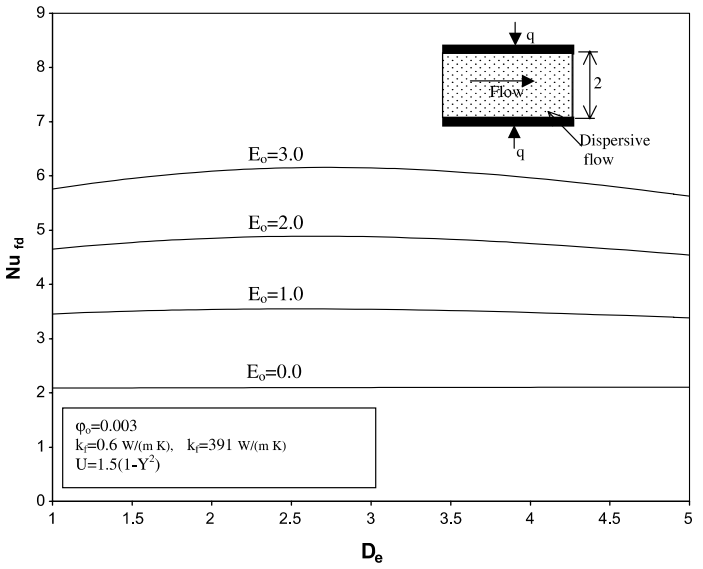

Fig. 13. Effects of D_e on the fully developed value for the Nusselt number (exponential distribution, the number of the dispersive elements is the same for each distribution).

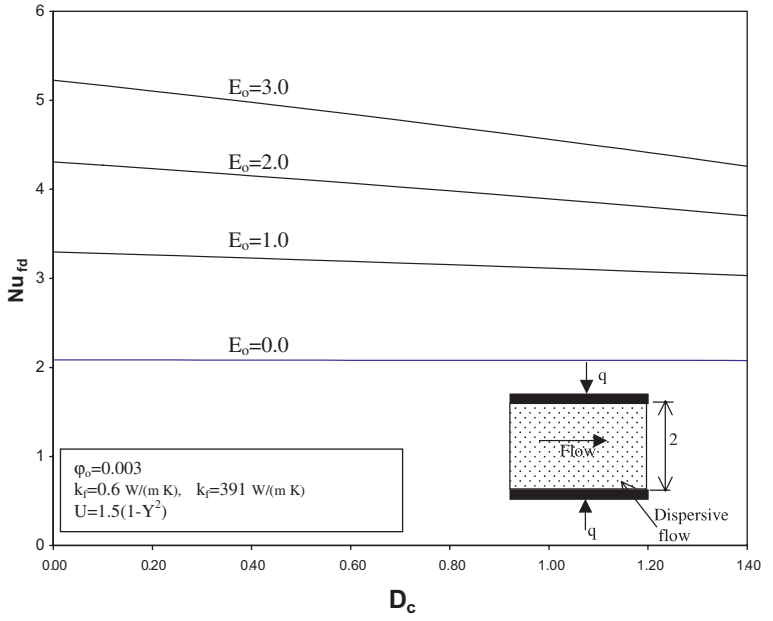

Fig. 14. Effects of D_c on the fully developed value for the Nusselt number (parabolic distribution, the number of the dispersive elements is the same for each distribution).

dispersive properties. Different distributions for dispersive elements such as nanoparticles or flexible hairy tubes extending from the channel plates are considered. The dispersive elements are considered to be uniformly distributed in the central region, near the boundaries, having an exponential distribution and having a parabolic distribution.

The boundary arrangement and the exponential distribution of the dispersive elements were shown to produce substantial enhancements in heat transfer compared to the case when the dispersive elements are uniformly distributed. The presence of the dispersive elements in core region produced no significant change in the heat transfer. The maximum excess in Nusselt

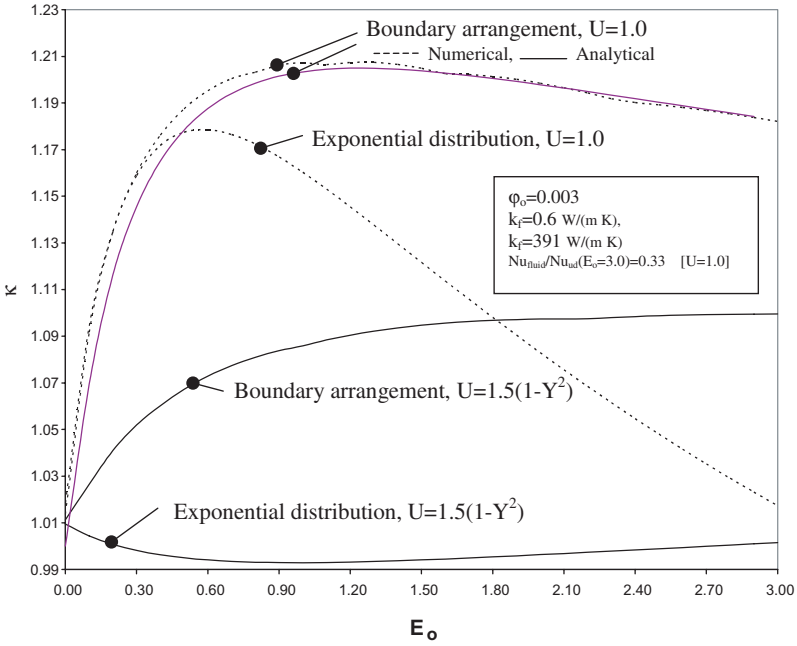

Fig. 15. Effects of the thermal dispersion parameter E_0 on the excess of Nusselt number for different arrangements (the number of the dispersive elements is the same for each distribution).

number was found to be 1.21 using the boundary arrangement for the volume fraction with uniform flow while the parabolic velocity profile produced a maximum excess in Nusselt number equal to 1.12. The volume fraction distribution that maximizes the heat transfer is governed by the flow and thermal conditions as well as the properties of dispersive elements. This work demonstrates that super nanofluids or super dispersive media can be prepared by controlling the thermal dispersion properties inside the fluid.

Acknowledgment

We acknowledge partial support of this work by DOD/DARPA/DMEA under grant number DMEA90-02-2-0216.

References

[1] K. Vafai, L. Zhu, Analysis of a two-layered micro channel heat sink concept in electronic cooling, International Journal of Heat and Mass Transfer 42 (1999) 2287–2297.

[2] M.B. Bowers, I. Mudawar, Two-phase electronic cooling using mini-channel and micro-channel heat sink, ASME Journal of Electronic Packaging 116 (1994) 290–305.

[3] K. Vafai, P.C. Huang, Analysis of heat transfer regulation and modification employing intermittently emplaced porous cavities, ASME Journal of Heat Transfer 116 (1994) 604–613.

[4] P.C. Huang, K. Vafai, Analysis of forced convection enhancement in a channel using porous blocks, AIAA Journal of Thermophysics and Heat Transfer 8 (1994) 563–573.

[5] A. Hadim, Forced convection in a porous channel with localized heat sources, ASME Journal of Heat Transfer 116 (1994) 465–472.

[6] A.-R.A. Khaled, K. Vafai, Cooling enhancements in thin films supported by flexible complex seals in the presence of ultrafine suspensions, ASME Journal of Heat Transfer 125 (2003) 916–925.

[7] A.-R.A. Khaled, K. Vafai, Nonisothermal characterization of thin film oscillating bearings in the presence of ultrafine particles, Numererical Heat Transfer, Part A 42 (2002) 549–564.

[8] K. Khanafer, K. Vafai, M. Lightstone, Buoyancy-driven heat transfer enhancement in a two-dimensional enclosure utilizing nanofluids, International Journal of Heat and Mass Transfer 46 (2003) 3639–3653.

[9] A. Ali, K. Vafai, A.-R.A. Khaled, Analysis of heat and mass transfer between air and falling film in a cross flow configuration, International Journal of Heat and Mass Transfer 47 (2004) 743–755.

[10] J.A. Eastman, S.U.S. Choi, S. Li, W. Yu, L.J. Thompson, Anomalously increased effective thermal conductivities of ethylene glycol-based nanofluids containing copper nanoparticles, Applied Physics Letters 78 (2001) 718–720.

[11] Y. Xuan, W. Roetzel, Conceptions for heat transfer correlation of nanofluids, International Journal of Heat and Mass Transfer 43 (2000) 3701–3707.

[12] P.Y. Chang, S.W. Shiah, M.N. Fu, Mixed convection in a horizontal square packed-sphere channel under axially uniform heating peripherally uniform wall temperature, Numerical Heat Transfer 45 (2004) 791–809.

[13] S. Hancu, T. Ghinda, L. Ma, D. Lesnic, D.B. Ingham, Numerical modeling and experimental investigation of the fluid flow and contaminant dispersion in a channel, International Journal of Heat and Mass Transfer 45 (2002) 2707–2718.
[14] A.V. Kuznetsov, L. Cheng, M. Xiong, Effects of thermal dispersion and turbulence in forced convection in a composite parallel-plate channel: investigation of constant wall heat flux and constant wall temperature cases, Numerical Heat Transfer 42 (2002) 365–383.
[15] D.J. Gunn, An analysis of convective dispersion and reaction in the fixed-bed reactor, International Journal of Heat and Mass Transfer 48 (2004) 2861–2875.
[16] T. Metzger, S. Didierjean, D. Maillet, Optimal experimental estimation of thermal dispersion coefficients in porous media, International Journal of Heat and Mass Transfer 47 (2004) 3341–3353.
[17] A. Amiri, K. Vafai, Analysis of dispersion effects and non-thermal equilibrium non-Darcian, variable porosity incompressible flow through porous medium, International Journal of Heat and Mass Transfer 37 (1994) 939–954.
[18] Q. Li, Y. Xuan, Convective heat transfer and flow characteristics of cu-water nanofluid, Science in China (Series E) 45 (2002) 408–416.
[19] F.J. Wasp, Solid–liquid Slurry Pipeline Transportation, Trans. Tech., Berlin, 1977.
[20] F.G. Blottner, Finite-difference methods of solution of the boundary-layer equations, AIAA Journal 8 (1970) 193–205.